

10. Ernst, E. J., Yodoi, K., Roling, E. E. and Klepser, M. E., Rates and extends of antifungal activities of Amphotericin B, Flucytosine, Luconazole, and Voriconazoles against *Candida lusitanae* determined by microdilution, estest and determined by time-kill methods. *J. Antimicrob. Agents Chemother.*, 2001, **46**, 578–581.
11. Baillie, G. S. and Douglas, L. J., Matrix polymers of *Candida* biofilms and their possible role in biofilm resistance to antifungal agents. *J. Antimicrob. Chemother.*, 2000, **46**, 397–403.
12. Hawser, S. P. and Douglas, L. J., Resistance of *Candida albicans* biofilms to antifungal agents *in vitro*. *Antimicrob. Agents Chemother.*, 1995, **39**, 2128–2131.
13. Chandra, J., Kuhn, D. M., Mukherjee, P. K., Hoyer, L. L., Cormick, T. Mc. and Ghannoum, M. A., Biofilm formation by the fungal pathogen *Candida albicans*: Development, architecture, and drug resistance. *J. Bacteriol.*, 2001, **183**, 5385–5394.
14. Cocuau, C., Rodier, M. H., Daniault, G. and Imbert, C., Antimetabolic activity of caspofungin against *Candida albicans* and *Candida parapsilosis* biofilms. *J. Antimicrob. Chemother.*, 2005, **56**, 507–512.
15. Al-Fattani, M. A. and Douglas, L. J., Penetration of *Candida* biofilms by antifungal agents. *Antimicrob. Agents Chemother.*, 2004, **48**, 3291–3297.
16. Samaranyake, Y. H., Ye, J., Yau, J. Y. Y., Cheung, B. P. K. and Samaranyake, L. P., *In vitro* method to study antifungal perfusion in *Candida* biofilms. *J. Clin. Microbiol.*, 2004, **43**, 818–825.
17. Kuhn, D. M., Chandra, J., Mukherjee, P. K. and Ghannoum, M. A., Comparison of biofilm formation *Candida albicans* and *Candida parapsilosis* on bioprosthetic surfaces. *Infect. Immunol.*, 2000, **70**, 878–888.
18. Kojie, E. M. and Darouchie, R. O., *Candida* infections of medical devices. *Clin. Microbiol. Rev.*, 2004, **17**, 255–267.
19. Mukherjee, P. K. and Chandra, J., *Candida* biofilm resistance. *Drug Resistance Updates*, 2004, **7**, 301–309.
20. Ramage, G., Walle, K. V., Wickes, B. L. and Lopez-Ribot, J. L., Standardized method for *in vitro* antifungal susceptibility testing of *Candida albicans* biofilms. *J. Antimicrob. Agents Chemother.*, 2001, **45**, 2475–2479.
21. Baillie, G. S. and Douglas, L. J., Iron limited biofilms of *Candida albicans* and their susceptibility to Amphotericin B. *Antimicrob. Agents Chemother.*, 1998, **42**, 2146–2149.
22. Garcí'a-Sa'ánchez, S., Aubert, S., Iraqui, S., Janbon, G., Ghigo, J. and d'Enfert, C., *Candida albicans* biofilms: A developmental state associated with specific and stable gene expression patterns. *Eukaryot. Cell.*, 2004, **3**, 536–545.
23. Hawser, S. P., Jessup, C., Vitullo, J. and Ghannoum, M. A., Utility of 2,3-bis(2-methoxy-4-nitro-5-sulfophenyl)-5-[phenyl-amino]carbonyl-2H-tetrazolium hydroxide (XTT) and minimum effective concentration assays in the determination of antifungal susceptibility of *Aspergillus fumigatus* to the lipopeptide class of compounds. *J. Clin. Microbiol.*, 2001, **39**, 2738–2741.
24. Ramage, G., Bachmann, S., Patterson, T. F., Wickes, B. L. and Lopez-Ribot, J. L., Investigation of multidrug efflux pumps in relation to fluconazole resistance in *Candida albicans* biofilms. *J. Antimicrob. Chemother.*, 2002, **49**, 973–980.
25. Gilfillan, G. D. Sullivan, D. J., Haynes, K., Parkinson, T., Coleman, D. C. and Gow, N. A. R., *Candida dubliniensis*: Phylogeny and putative virulence factors. *Microbiology*, 1998, **144**, 829–838.
26. McCourtie, J. and Douglas, L. J., Relationship between cell surface composition, adherence, and virulence of *Candida albicans*. *Infect. Immunol.*, 1984, **45**, 6–12.
27. Odds, F. C., Gow, N. A. R. and Brown, A. J. P., Fungal virulence studies come of age. *Genome Biol.*, 2004, **2**, 1009.1–1009.4.
28. Ramage, G. Saville, S. P., Thomas, D. P. and Lopez-Ribot, J. L., *Candida* biofilms: An update. *Eukaryot. Cell*, 2005 **4**, 633–638.

## Clay mineralogical studies of sediments and strontium isotope analyses on calcretes at the prehistoric site of Attirampakkam, Tamil Nadu

Arun K. Sreedhar<sup>1</sup>, S. Balakrishnan<sup>1\*</sup>,  
Shanti Pappu<sup>2</sup> and Kumar Akhilesh<sup>2</sup>

<sup>1</sup>Department of Earth Sciences, Pondicherry University,  
Puducherry 605 014, India

<sup>2</sup>Sharma Centre for Heritage Education, Chennai 600 004, India

**Archaeological excavations at the Palaeolithic site of Attirampakkam, Tiruvallur District, Tamil Nadu, yielded artefacts dating to the Lower and Middle Palaeolithic cultural phases assigned to the Middle to Late Pleistocene. This communication reports preliminary results of clay mineral analysis, which suggests the influence of both provenance and climate during the Pleistocene. The higher <sup>87</sup>Sr/<sup>86</sup>Sr values suggest chemical weathering of silicate minerals present in the host sediments as the predominant source for Ca in the calcretes.**

**Keywords:** Calcretes, clay mineralogy, palaeoclimate, sediments, strontium isotopes.

THE prehistoric site of Attirampakkam forms one of a complex of numerous Palaeolithic archaeological sites of northern Tamil Nadu<sup>1</sup>. Excavations were conducted at this site (under the direction of S.P.)<sup>2-5</sup>, aimed at understanding hominin-adaptive strategies over the Middle to Late Pleistocene in relation to past environments. A notable feature at the site was the presence of a continuous stratified sequence of Palaeolithic industries ranging from the Lower Palaeolithic (Acheulian) to the Middle Palaeolithic, signifying long-term occupation of the site.

This communication presents a preliminary analysis of the variation in clay mineralogy in the sequence studied, identifies the source for Ca in the calcrete lenses or nodules noted in all layers, and reports inferences on possible climatic changes. The study of clay minerals<sup>6-9</sup> indicates that their formation depends on climatic as well as geological and topographical features of a region<sup>10</sup>. Clay minerals are commonly used to determine the type and intensity of weathering processes<sup>11</sup>. Calcium carbonate concretions known as calcretes are widespread in arid and semi-arid climate, and strontium (Sr) isotopes are used as tracers to determine the provenance of Ca sources<sup>12</sup>.

The site of Attirampakkam (locally known as Manamedu; 13°13'50"N and 79°53'20"E) is situated less than 1 km from the River Kortallayar, Tiruvallur District, Tamil Nadu (Figure 1). Annual rainfall of 96 cm was recorded for Chennai, whereas the study area, located about 50 km

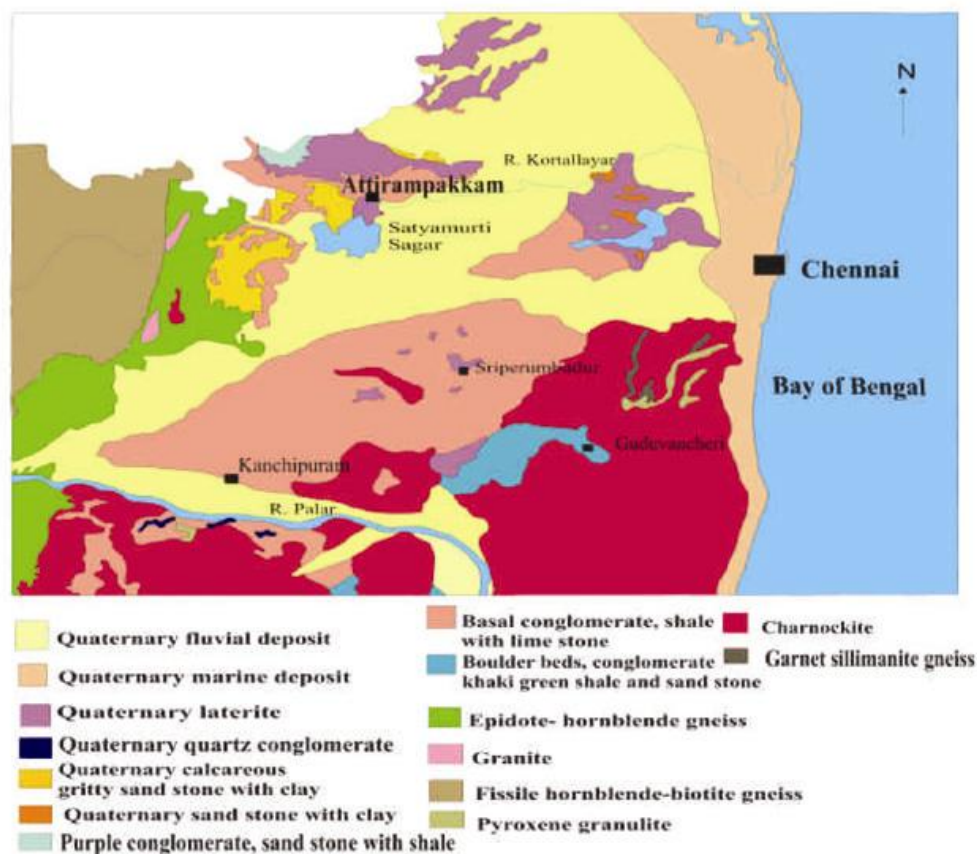


Figure 1. Geological map of the area around Chennai with the location of the Palaeolithic site of Attirampakkam<sup>31</sup>.

west, receives lower rainfall compared to Chennai. The regional topography comprises the NNE–SSW-trending Allikulli Hills (200–380 m asl) lying to the west of Attirampakkam. These are uplifted and well-preserved palaeodeltas of early Cretaceous age<sup>13–16</sup>. The cobble conglomerate in the Allikulli Hills was sourced from the quartzitic Cuddapah ranges of Mesoproterozoic age to the west. The lower-lying areas of the piedmont are underlain by shaly marine sediments of the Avadi Formation. Being coeval and intertonguing with the conglomerate beds, it may represent the palaeodelta bottomset beds. The shales are capped by Tertiary laterites. During the excavation, six sedimentary units were recognized, comprising a laminated argillaceous bed (layer 6), disconformably overlain by a thick sequence of ferricretes in a silty matrix (layer 5), which was capped by clayey-silt (layers 3 and 4). These were overlain by ferricretes supported by silty matrix (layer 2) and argillaceous colluvium (layer 1). Acheulian industries were noted in layer 6, with a Late Acheulian in layer 5 and industries transitional to the Middle Palaeolithic in layers 3 and 4. Middle Palaeolithic assemblages were noted in layer 2 of this site.

The most important aspect of the site is presence of a stratified sequence of cultural phases, indicating long-

term occupation of the site over the Middle to Late Pleistocene. Further, the discovery of Lower Palaeolithic Acheulian artefacts within layer 6, which was previously termed the Avadi or Sriperumbudur Formation (Cretaceous), was unique. This led to the revision about understanding the local geology and geomorphological features of this area. Variability in the assemblage structure through time, when studied along with regional archaeological record, also indicates movement of prehistoric populations across the landscape and pointed to the varied ways in which this site was used through time. The importance of this research also lies in the use of multidisciplinary scientific approaches towards addressing research questions<sup>1–5</sup>.

A total of 31 samples were collected vertically downwards at intervals of 10 cm from the west wall of the trench T7A (Figure 2). Three samples were also collected from the *in situ* Avadi shale in the gully near the village of Attirampakkam. From each sample, 50 g was removed for clay mineral analysis after coning and quartering. The samples were subjected to ultrasound treatment for about 10 min; and silt- and clay-sized fractions were separated from the coarser fractions by wet-sieving using ASTM 230 mesh. Further clay mineral separation was carried out

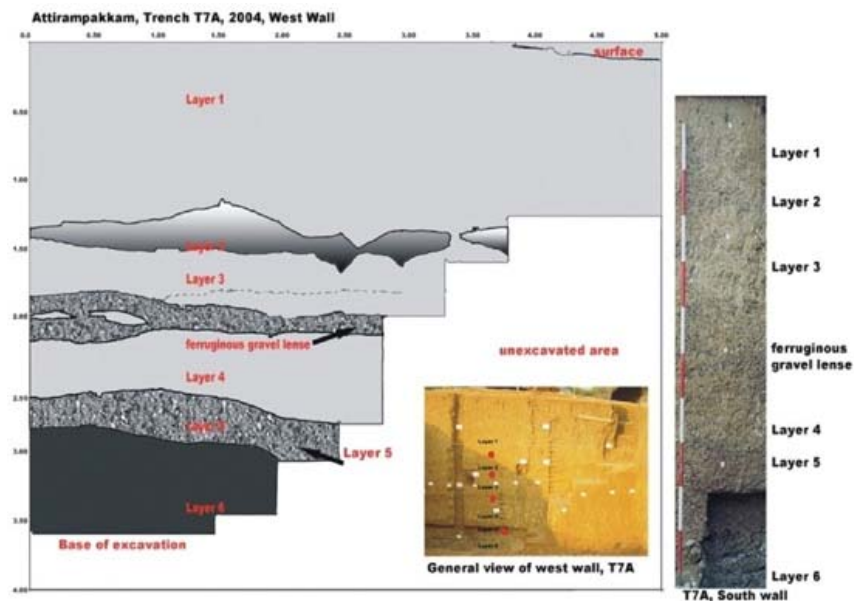


**Figure 2.** Photograph of west wall and south wall of trench T7A at Attirampakkam. Various layers of the west wall are delineated based on nature of sediments and artefacts found in them.

using settling columns following procedures detailed in Deepthy and Balakrishnan<sup>17</sup>. The separated clay minerals were saturated with KCl and CaCl<sub>2</sub> solutions to homogenize the interlayer cations. Subsequently, slides were prepared by pipetting out a few drops onto a glass slide. The samples treated with KCl underwent different heat treatments: 130°C (12 h), 300°C (4–5 h) and 550°C (3 h). Glycolation was done on samples treated with CaCl<sub>2</sub> (at 60°C for 8 h).

Samples were analysed using an X'pert PRO PANalytical X-ray diffractometer equipped with  $\theta$ - $\theta$  type goniometer, at the Department of Earth Sciences, Pondicherry University. The samples were scanned between 2 and 30° 2 $\theta$  with a speed of 0.01 (°/s), and at 40 kV acceleration voltage and 25 mA current. Clay minerals were identified adopting standard procedures<sup>18–20</sup>.

Six calcrete samples were collected from each of the six sedimentary units of trench T7A. About 100 mg of these samples was placed in a Teflon<sup>®</sup> beaker, washed with double-distilled water, and subsequently subjected to ultrasound treatment for 15 min. The residues were collected and the above processes were repeated four times to remove surface contaminations. The dried samples were weighed in an electronic balance and 1 ml of 1 M acetic acid was added. These were then left for 12 h to complete the reaction. The samples were then passed through filter paper and the clear solutions representing CaCO<sub>3</sub> were dried. Two millilitres of double-distilled 2N HCl was added to the samples and passed twice through cation exchange columns to concentrate Sr. A few samples of sediments that host calcretes were also taken to study the isotope composition of exchangeable Sr. Extraction of

exchangeable Sr was carried out following the procedure outlined by Bullen *et al.*<sup>21</sup>. Sr isotope composition was measured using a Thermal Ionization Mass Spectrometer, at the Department of Earth Sciences, Pondicherry University.

Kaolinite, smectite and clay-mica are present in stratigraphic layer 1 (argillaceous colluvium; archaeologically sterile) and layer 6 (laminated argillaceous bed; Acheulian); whereas layer 2 (ferricretes in a silty matrix; Middle Palaeolithic), layers 3 and 4 (clayey-silts; transitional between Lower and Middle Palaeolithic) and layer 5 (ferricretes in a silty matrix; Late Acheulian to Early-Middle Palaeolithic) contain only kaolinite and clay-mica. However, comparatively higher percentage of smectite is noted within sections of layers 3 and 4 (2.1–2.2 m). Clay minerals such as kaolinite, smectite and clay-mica predominate the original Avadi shales, which constitute the pre-Pleistocene bedrock in the region.

The major clay minerals present in the samples are kaolinite, smectite and clay-mica. Kaolinite was identified using 7 and 3.5 Å peaks. These peaks disappeared on heating to 550°C. Smectite was identified by a 15 Å peak, which shifted to 17 Å on glycolation. The 10 Å peak, represented by clay mica, remained as such up to 550°C (Figures 3 and 4). The relative percentage of clay minerals was calculated using the relation:

$$\text{Relative percentage} = \frac{I_{001} \text{ clay mineral}}{\sum I_{001} \text{ all clay minerals}} \times 100,$$

where  $I_{001}$  is the intensity of the 001 peak.

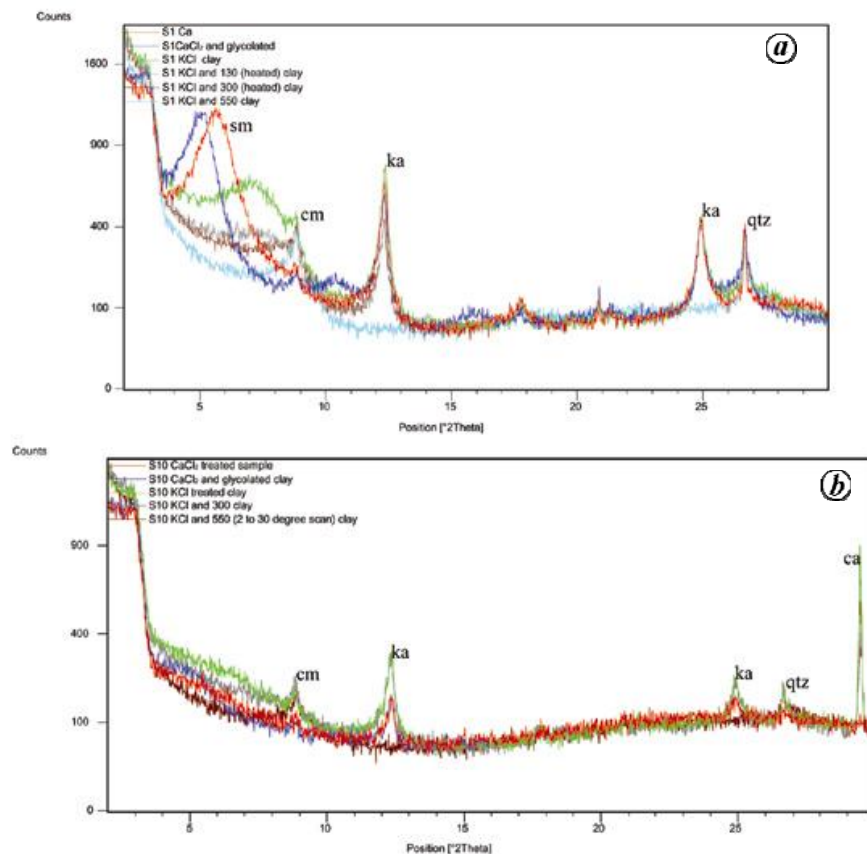


**Figure 3.** *a*, X-ray diffraction pattern of samples from layer 1, which have significant quantities of the clay mineral smectite. Clay fractions of the samples were subjected to various treatments for identification of clay minerals. The 15 Å peak of smectite shifted to 17 Å on glycolation. There is not much variation in the intensity of the kaolinite peak with increase in temperature up to 300°C; however, its peak disappeared at 550°C. The 10 Å peak remains as such even after heating to a temperature of 550°C, suggesting that the mineral is clay mica. *b*, Clay mineralogy of layers such as 2–5 which contain kaolinite and clay-mica, but not smectite. sm, Smectite; ka, Kaolinite; cm, Clay mica; qtz, Quartz and ca, Calcite.

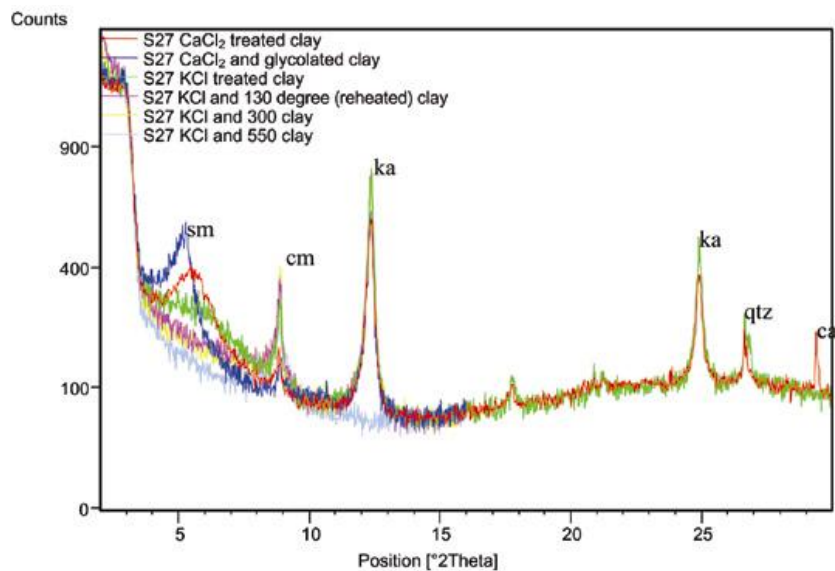


**Figure 4.** X-ray diffraction pattern of samples from layer 6 in which smectite appears at a depth of 2.9 m. However, the intensity of the smectite peak is lower compared to layer 1.

Among the CaCl<sub>2</sub> and KCl-treated samples, the strongest peak was selected for relative percentage calculations for the clay mineral of interest. The clay mineralogical compositions and their relative percentages in each sample are given in Table 1.

At surface pressure and temperature conditions, most clay minerals are the result of an incongruent dissolution of silicate minerals during weathering<sup>22</sup>. As suggested by Tardy *et al.*<sup>23</sup>, the alteration of primary minerals such as biotite and plagioclase can produce smectite under semi-arid climate. If there is low rainfall, the water/rock ratio decreases. As a result, Si<sup>4+</sup> ion concentration and metals/H<sup>+</sup>

ratio come into equilibrium with the rock. Under this condition K<sup>+</sup>/H<sup>+</sup>, Na<sup>+</sup>/H<sup>+</sup>, Ca<sup>2+</sup>/H<sup>+</sup> and Mg<sup>2+</sup>/H<sup>+</sup> ratios increase, which favours the formation of smectite on weathering of silicate minerals<sup>22</sup>. Clay-mica can also form by alteration of muscovite and biotite.

Rainfall exceeding 100 cm results in higher water/rock ratio, which lowers the Si<sup>4+</sup> ion concentration, as well as metals/H<sup>+</sup> ratio. This will favour the formation of kaolinite directly from silicate minerals. Extremely low Si and metals/H<sup>+</sup> ratio result in the formation of gibbsite and goethite<sup>17,22,24</sup>. Based on detailed clay mineralogy of weathering profile developed on either side of Western Ghats, India, it has been suggested that with sufficiently higher rainfall, kaolinite will develop irrespective of silicate rock composition<sup>17</sup>.

Various studies<sup>10,24</sup> have empirically determined that kaolinite forms when the mean annual precipitation (MAP) is above 50 cm, while smectite will be dominant when MAP is below 100 cm. Occurrence of both kaolinite and smectite in the weathering profile could indicate rainfall between 50 and 100 cm (MAP). On the other hand, presence of only kaolinite in some layers may suggest that rainfall was more than 100 cm.

In terms of both clay mineralogy and appearance, layer 6 sediments are similar to the original *in situ* Avadi shale (Figure 5) and were termed as such by previous researchers<sup>2</sup>. The presence of numerous Lower Palaeolithic Acheulian tools within sediments of layer 6 led to the interpretation that these sediments represent Pleistocene floodplain deposits of fluvial origin, consisting of re-worked Avadi shales, inevitably containing some of its original foraminiferas. Layer 6 aggraded during site occupation and therefore corresponds to Acheulian horizons<sup>5</sup>; further studies are in progress regarding this aspect.

**Table 1.** Depth, stratigraphy and clay mineralogical information of samples collected from the west wall of the trench T-7A at Attirampakkam

Sample no.	Depth (cm)	Layer	Clay mineral assemblages with relative percentages		
			sm	ka	cm
S1	30	1	52.4	35	12.5
S2	40	1	49.3	44	6.6
S3	50	1	59.9	29.2	10.9
S4	60	1	55.5	37.6	7
S5	70	1	31.6	42.9	25.5
S6	80	1	35	48.6	16.3
S7	90	1	22.8	57.8	19.4
S8	100	1	31.4	58	19.4
S9	110	1	28.8	60.5	10.7
S10	120	2	–	86.5	13.5
S11	130	2	–	50.9	49
S12	140	2	–	74.5	25.5
S13	150	3	–	95.4	4.6
S14	160	3	–	68.3	31.7
S15	170	3	–	90.1	9.9
S16	180	3	–	88.4	11.6
S17	190	3	–	54.6	45.4
S18	200	3	–	70.3	29.7
S19	210	3	18.2	63.7	18.1
S20	220	4	19	66.2	14.6
S21	230	4	–	82.9	17
S22	240	4	–	79.5	20.5
S23	250	4	6.2	75.7	18
S24	260	4	–	80.8	19.2
S25	270	5	–	47.3	52.7
S26	280	5	–	89.3	10.7
S27	290	6	17.5	69.4	13
S28	300	6	35	60.3	5
S29	310	6	38.2	41	21
S30	320	6	40.8	49.5	9.7
S31	330	6	34.3	45.6	20
AV1	83	–	48	44.4	8
AV2	158	–	48.2	36.7	15
AV3	210	–	41.6	26	32.3

ka, Kaolinite; sm, Smectite; cm, Clay-mica and AV, Avadi shale.

Layer 1: Argillaceous colluvium (archaeologically sterile).

Layer 2: Ferricrete-rich layer (Middle Palaeolithic).

Layers 3 and 4: Clayey-silts (Middle Palaeolithic transitional from Acheulian).

Layer 5: Ferricrete-rich layer (Late Acheulian to Early Middle Palaeolithic).

Layer 6: Laminated argillaceous bed (Acheulian).

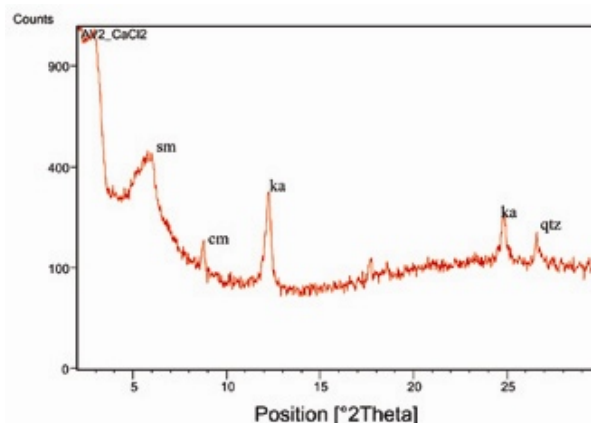


**Figure 5.** X-ray diffraction pattern of a sample of the Avadi shale collected from Attirampakkam gully. Totally three samples are studied, and all have identical clay mineral assemblage of kaolinite, smectite and clay mica. The clay-mineral assemblage of samples of Avadi shale is similar to that observed for the layers 1 and 6 of the Palaeolithic site.

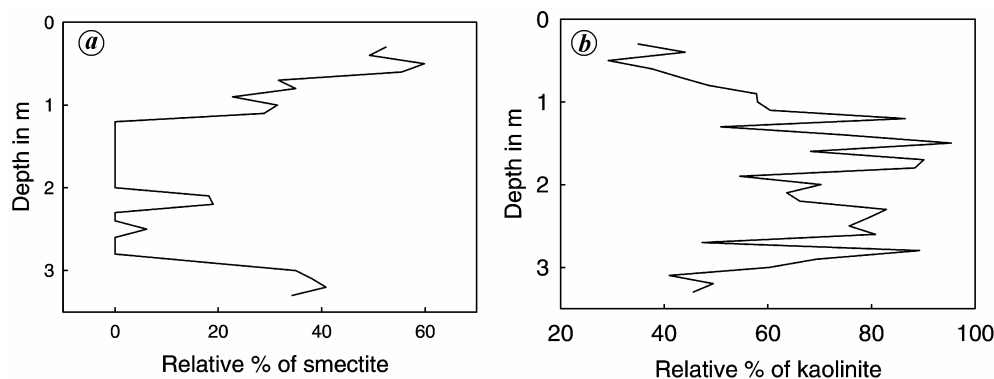


**Figure 6.** *a*, Relative percentage of smectite vs depth plotted for sediment samples from Attirampakkam. Smectite is higher in the top 1.1 m (layer 1) depth. Between 1.2 and 2.8 m depth, smectite is absent, although it appears between 2.1 and 2.2 m depth just below a lens of ferricrete sediments. Further, below 2.9 m depth (layer 6), the relative percentage of smectite steadily increases, but is comparatively less than that of layer 1. *b*, Kaolinite is present in all layers but the relative percentage is higher at depths ranging between 1.2 and 2.8 m (layers 2–5).

**Table 2.**  $^{87}\text{Sr}/^{86}\text{Sr}$  values of calcretes, soil leachates and their depth

Sample no.	Depth (cm)	$^{87}\text{Sr}/^{86}\text{Sr}$	$^{87}\text{Sr}/^{86}\text{Sr}$ of leachates
S2L1	40	$0.713908 \pm 8$	$0.714768 \pm 6$
S211L2	130	$0.715022 \pm 7$	–
S15L3	170	$0.714609 \pm 5$	–
S22L4	240	$0.715856 \pm 4$	$0.715551 \pm 4$
S26L5	280	$0.715288 \pm 4$	–
S30L6	320	$0.714979 \pm 9$	$0.715467 \pm 5$

S, Sample number; L, layer number.

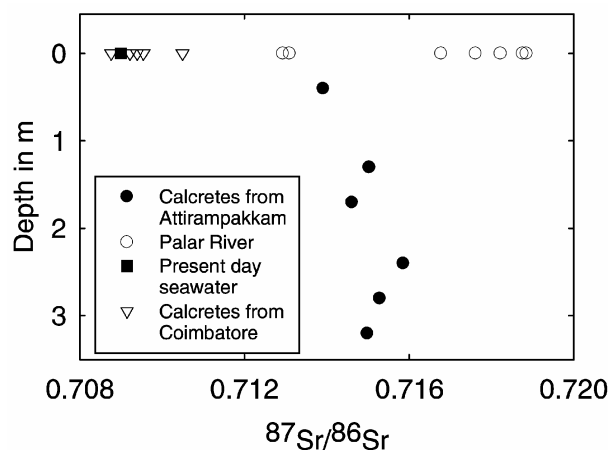


**Figure 7.**  $^{87}\text{Sr}/^{86}\text{Sr}$  ratios measured on calcretes from Attirampakkam plotted against depth where calcretes occur. Note that  $^{87}\text{Sr}/^{86}\text{Sr}$  ratios of calcretes fall within the range of Sr isotope ratio of the Palar river water samples. Sr isotope ratio of present-day sea water<sup>29</sup>,  $0.70910 \pm 4$ , and  $^{87}\text{Sr}/^{86}\text{Sr}$  ratios of calcretes from Coimbatore<sup>26</sup> area are also shown for comparison.

If Avadi shales were reworked and deposited as layer 6 under more humid climate with MAP exceeding 100 cm, then smectite + kaolinite assemblage present in the Avadi

shale should have undergone further chemical weathering to give kaolinite ± goethite ± gibbsite assemblage. Whereas, both the Avadi shale and layer 6 contain smectite + kaolinite assemblage, which indicates a semi-arid climate, with MAP less than 100 cm at the time of deposition of layer 6.

Predominance of smectite and kaolinite in the top 1.1 m of the deposit comprising layer 1 (archaeologically sterile), suggests deposition under a semi-arid climate with MAP below 100 cm (Figure 6), and therefore, similar to the present-day climate or slightly drier.

Differences in clay mineral assemblage between layers 1 and layers 2–5, could be explained by differences in provenance and derivation of sediments from sources that had similar differences in clay mineral content as noted in other studies<sup>2–5</sup>. However, even accounting for differences in provenance, clay minerals during deposition are expected to undergo transformation to remain in equilibrium with the prevalent climatic conditions. In this context timescale of deposition of these Pleistocene sediments is an important factor to be taken into consideration to firmly establish the relationship between climate and clay mineralogy, and results of the OSL, palaeomagnetic and cosmogenic Be studies are awaited.

The formation of calcrete is common under arid and semi-arid conditions<sup>25,26</sup>, which are ideal for the precipitation of  $\text{CaCO}_3$ . The calcrete forms through evaporative precipitation of water in phreatic and capillary fringe environments. Since Sr can replace Ca in mineral structures, it can be used as a tracer for the source of Ca<sup>27,28</sup>. Calcretes noted in layers 1–6 exhibit  $^{87}\text{Sr}/^{86}\text{Sr}$  ratios between  $0.715856 \pm 4$  and  $0.713908 \pm 8$  (Table 2).

Durand *et al.*<sup>26</sup> have reported that the calcretes near Coimbatore, Tamil Nadu have  $^{87}\text{Sr}/^{86}\text{Sr}$  ratios similar to the present-day seawater, and considered that Ca and Sr of the calcretes were derived from marine sources. Whereas the  $^{87}\text{Sr}/^{86}\text{Sr}$  ratios of the Attirampakkam cal-

cretes are higher than the marine values and close to those reported for the lower reaches of Palar (Figure 7) flowing through granulites, Lower Gondwana formations and Recent alluvium. The  $^{87}\text{Sr}/^{86}\text{Sr}$  ratios of the calcretes are lower than those of the upper reaches of Palar river (Figure 7). Hence, there is a possibility that Sr and Ca found in calcretes could have been derived from two distinct sources.

The  $^{87}\text{Sr}/^{86}\text{Sr}$  ratio of leachates of sediments that host the calcretes needs to be taken into consideration while modelling relative contributions of Sr from the sediments. Their  $^{87}\text{Sr}/^{86}\text{Sr}$  ratios vary between  $0.71551 \pm 4$  and  $0.714768 \pm 6$  (Table 2), and the relatively more radiogenic Sr isotope composition of the leachates is a result of alteration and release of Sr by silicate minerals with high Rb/Sr ratio derived from Precambrian rocks. The most radiogenic value of the leachates is considered as one end member and the other end member is that of marine carbonates of Upper Cretaceous age (0.708375). To quantify the contributions, two-component mixing calculation<sup>29,30</sup> was done and the results are shown in Figure 8.

The calcretes plot to the left of the mixing line between seawater and leachate because Sr abundance in the calcretes is much higher (400–800  $\mu\text{g/g}$ ), while the sea water and leachates have 8 and 6  $\mu\text{g/g}$  Sr respectively. However, the Sr isotope composition of calcrete could be compared with the mixing line to infer the relative contributions. Calcrete in layer 1 received ca. 20% contribution from marine sources and the remaining 80% input from water interacting with the sediments. Calcretes from layers 3, 6, 2, 5 and 4 have progressively higher Ca and Sr contribution, ca. 90–100%, by leaching of the sedi-

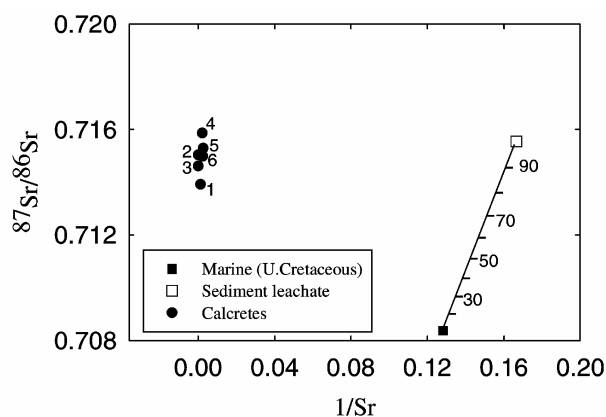


**Figure 8.** Mixing line calculated for two-component mixing involving marine source (Upper Cretaceous) and sediment leachates. The calcretes contain higher concentration of Sr (400–800  $\mu\text{g/g}$ ) than sea water (8  $\mu\text{g/g}$ ) and sediment leachates (6  $\mu\text{g/g}$ ), and therefore, they fall on the left side of the two-component mixing line. However, the relative contribution could be inferred by horizontal shifting of the mixing line close to the calcrete data. It is clear that calcretes from layer 1 received ca. 20% Ca and Sr from marine sources and 80% from the weathering of sediments that host calcretes, while for rest of the samples 90–100% input was derived by the leaching of sediments.

ments. Hence, it is inferred that Ca and Sr were predominantly derived from percolating water in the vadose zone, which interacted with the sediments to form calcretes.

Attirampakkam is an important example of an open-air Palaeolithic site in India, occupied for a long time-period, with variability noted in the prehistoric assemblage structures marking changing hominin behaviour patterns.

Based on clay mineralogy of sediments of various layers, it is inferred that during the Acheulian period (layer 6), the Attirampakkam site experienced semi-arid climate with MAP < 100 cm, which changed to more humid climate with MAP > 100 cm throughout Late Acheulian to Middle Palaeolithic periods (layers 5–2). The archaeologically sterile layer 1 was deposited under semi-arid conditions as that of present day. From the Sr isotope composition of calcretes compared to the two-component mixing model involving sediment leachates and marine sources, it is inferred that Sr as well as Ca were predominantly derived by water–sediment interactions in the vadose zone of the Pleistocene deltaic sediments of this site. Further studies are in progress, which will aid in providing a better understanding of past climatic conditions and hominin response during the Pleistocene epoch at this site.

1. Pappu, S., *A Re-examination of the Palaeolithic Archaeological Record of Northern Tamil Nadu, South India*, BAR-International Series-1003, Oxford, 2001.
2. Pappu, S., Gunnell, Y., Taieb, M., Brugal, J.-P. and Touchard, Y., Ongoing excavations at the Palaeolithic site of Attirampakkam, South India: Preliminary findings. *Curr. Anthropol.*, 2003, **44**, 591–597.
3. Pappu, S., Gunnell, Y., Taieb, M., Brugal, J.-P., Anupama, K., Sukumar, R. and Kumar, A., Excavations at the Palaeolithic site of Attirampakkam, South India. *Antiquity*, 2003, **77**, 297.
4. Pappu, S., Gunnell, Y., Taieb, M. and Kumar, A., Preliminary report on excavations at the Palaeolithic site of Attirampakkam, Tamil Nadu (1999–2004). *Man Environ.*, 2004, **XXIX**, 1–17.
5. Gunnell, Y., Rajashekar, C., Pappu, S., Taieb, M. and Kumar, A., On the depositional environment of lower Palaeolithic horizons at the prehistoric site of Attirampakkam, Tamil Nadu. *Curr. Sci.*, 2006, **91**, 114–118.
6. Chamley, H., *Clay Sedimentology*, Springer-Verlag, Berlin, 1989.
7. Sharma, A. and Rajamani, V., Major element, REE, and other trace element behavior in amphibolites weathering under semiarid conditions in southern India. *J. Geol.*, 2000, **8**, 487–496.
8. Keller, W. D., Environmental aspects of clay minerals. *J. Sediment Petrol.*, 1970, **40**, 788–813.
9. Chaudhri, S. and Kalitha, C. K., X-ray study of clay mineralogy of Krolo Formation of the Mussoorie Hills, Kumaon Himalaya, India. *J. Earth Sci.*, 1985, **12**, 239–248.
10. Singer, A., The paleoclimatic interpretation of clay minerals in sediments – A review. *Earth Sci. Rev.*, 1984, **21**, 251–293.
11. Thamban, M., Purnachandra Rao, V. and Schneider, R. R., Reconstruction of late Quaternary monsoon oscillations based on clay mineral proxies using sediment cores from the western margin of India. *Mar. Geol.*, 2002, **186**, 527–539.
12. Chiquet, A., Michard, A., Nahon, D. and Hamelin, B., Atmospheric input vs *in situ* weathering in the genesis of calcretes: An Sr isotope study at Galvez (Central Spain). *Geochim. Cosmochim. Acta*, 1999, **63**, 311–323.

13. Pappu, S., Reinvestigation of the prehistoric archaeological record in the Kortallayar Basin, Tamil Nadu. *Man Environ.*, 1996, **XXI**, 1–23.
14. Pappu, S., A study of natural site formation processes in the Kortallayar Basin, Tamil Nadu, South India. *Geoarchaeol. Int. J.*, 1999, **14**, 127–150.
15. Muralidharan, P. K., Prabhakar, A. and Kumaraguru, P., In Workshop on Evolution of East Coast of India, Abstr., Tamil University, Tanjore, 18–20 April 1993.
16. Kumaraguru, P. and Trivikrama Rao, A., A reappraisal of the geology and tectonics of the Palar basin sediments, Tamil Nadu. In Ninth International Gondwana Symposium, Hyderabad, Geological Survey of India and Balkema, Rotterdam, 1994, vol. 2, pp. 821–831.
17. Deepthy, R. and Balakrishnan, S., Climate control on clay mineral formation: Evidence from weathering profiles developed on either side of the Western Ghats. *J. Earth Syst. Sci.*, 2005, **114**, 1–12.
18. Dixon, J. B. *et al.*, *Minerals in Soil Environments*, Soil Science Society of America, 1977.
19. Brindley, G. W. and Brown, G., *Crystal Structures of Clay Minerals and their X-Ray Identification*, Mineralogical Society of London, Monograph No. 5, 1980.
20. Nesse, W. D., *Introduction to Mineralogy*, Oxford University Press, New York, 2000.
21. Bullen, T., White, A., Blum, A., Harden, J. and Schulz, M., Chemical weathering of a soil chronosequence on granitoid alluvium: Mineralogic and isotopic constraints on the behavior of strontium. *Geochim. Cosmochim. Acta*, 1997, **61**, 291–306.
22. Velde, B., *Introduction to Clay Minerals*, Chapman & Hall, London, 1992.
23. Tardy, Y., Bocquier, G., Paquet, H. and Millot, G., Formation of clay from granite and its distribution in relation to climate and topography. *Geoderma*, 1973, **10**, 271–284.
24. Birkeland, P. W., *Soils and Geomorphology*, Oxford University Press, New York, 1999.
25. Singer, A., The paleoclimatic interpretation of clay minerals in soils and weathering profiles. *Earth Sci. Rev.*, 1980, **15**, 303–326.
26. Durand, N., Gunnell, Y., Curmi, P. and Ahmad, S. M., Pathways of calcareous development on weathered silicate rocks in Tamil Nadu, India: Mineralogy, chemistry and paleoenvironmental implications. *Sediment. Geol.*, 2006, **192**, 1–18.
27. Khadkikar, A. S., Elemental composition of calcites in late Quaternary pedogenic calcaretes from Gujarat, western India. *J. Asian Earth Sci.*, 2005, **25**, 893–902.
28. Tripathi, J. K., Bock, B., Rajamani, V. and Eisenhauer, A., Ca and Sr dynamics in the Indo-Gangetic plains: Different sources and mobilization processes in northwestern India. *Curr. Sci.*, 2004, **87**, 1453–1458.
29. Faure, G., *Principles of Isotope Geology*, John Wiley, New York, 1986.
30. Pattanaik, J. K., Balakrishnan, S., Bhutani, R. and Singh, P., Chemical and strontium isotopic composition of Kaveri, Palar and Ponnaiyar rivers: Significance to weathering of granulites and granitic gneisses of southern Peninsular India. *Curr. Sci.*, 2007, **93**, 1–9.
31. Geological Survey of India, Geological and mineral map of Tamil Nadu and Pondicherry, 1995.

**ACKNOWLEDGEMENTS.** S.P. and K.A. thank the Archaeological Survey of India and Department of Archaeology, Government of Tamil Nadu for issuing permits for the excavation; Sharma Centre for Heritage Education, Chennai for logistic support; and the Homi Bhabha Fellowships Council; Leakey Foundation, USA, and Earthwatch Institute, USA, for funding various stages of the excavation project. We thank the staff of Sharma Centre for Heritage Education, students from various universities and villagers of Manamedu for their contribution to the

project. We also thank the reviewers for their comments which were useful in revising the manuscript. S.B. thanks DST, New Delhi for funds through a National Facility project and A.K.S. is grateful to CSIR, New Delhi for providing Junior Research Fellowship.

Received 11 April 2007; revised accepted 28 January 2008

## Evidences and radiocarbon ( $^{14}\text{C}$ ) ages of palaeo-high sea-level position around Mandapam, southeast coast of India

G. Gaitan Vaz<sup>1,2,\*</sup>, M. Hariprasad<sup>2</sup> and B. R. Rao<sup>1</sup>

<sup>1</sup>Operation: East Coast-II, Marine Wing, Geological Survey of India, Visakhapatnam 530 018, India

<sup>2</sup>Present address: Operation: West Coast-II, Marine Wing, GSI, Fourth Floor, 'C' Block, Kendriya Bhavan, Kakanad, Cochin 682 037, India

**A well-laminated, cross-bedded and coarse to very coarse-grained calcareous (beach rock) sandstone unit is exposed on either sides of Mandapam foreland along the Palk Bay and the Gulf of Mannar coasts at about 2 m asl. Presence of abundant coral debris and pelecypod shells in the sandstone indicates its formation under high-energy beach facies. Coral debris *Acropora* sp. and pelecypod shells, *Arca* sp. in living positions collected from the sandstone unit yielded  $^{14}\text{C}$  ages of 6110 and 5650 yrs BP respectively. The level of occurrence of calcareous sandstone and  $^{14}\text{C}$  ages of coral debris and pelecypod shells confirm that the mid-Holocene high strandline stood at about 2 m asl in this coastal segment between 5650 and 6110 yrs BP.**

**Keywords:** Beach rock, palaeo-high sea-level, radiocarbon ages, sandstone unit.

THE thrust on the study of past, present and future sea-level positions is gaining momentum worldwide because it concerns not only earth scientists, but climatologists, glaciologists, biologists, environmentalists, city and town planners, administrators, etc. In India, along the coastal areas, evidences of palaeo-high sea-level positions from the Pleistocene onwards are well established by remote-sensing studies followed by ground-truth collection. The datable materials collected from the palaeo-high sea-level positions from western and eastern coastal segments have yielded  $^{14}\text{C}$  ages between 120,000 and 5100 yrs BP. These  $^{14}\text{C}$  ages reveal that the Holocene sea level reached a maximum between 6500 and 5100 yrs BP.

\*For correspondence. (e-mail: ggaitanvaz@rediffmail.com)